ADVANCED FUNCTIONAL MATERIALS
www.afm-journal.de

Growth of a Highly Porous Coordination Polymer on a Macroporous Polymer Monolith Support for Enhanced Immobilized Metal Ion Affinity Chromatographic Enrichment of Phosphopeptides

*Adeela Saeed, Fernando Maya, Dianne J. Xiao, Muhammad Najam-ul-Haq, Frantisek Svec, and David K. Britt**

A simple room temperature solution-based method for the preparation of highly porous iron(III) benzenetricarboxylate coordination polymer films on the internal surface of a macroporous polystyrene-divinylbenzene-methacrylic acid polymer is reported. The resulting metal-organic polymer hybrid (MOPH) maintains a high specific micropore surface area of 389 $m^2 g^{-1}$ and thermal stability above 250 °C in air. The MOPH preparation is readily adapted to a capillary column, yielding a flow-through separation device with excellent flow permeability and modest back-pressure. The excellent separation capability of the MOPH column is demonstrated by enriching phosphopeptides from mixtures of digested proteins. This approach to MOPH synthesis is easily implemented and likely adaptable to a wide range of coordination polymers and metal-organic frameworks.

1. Introduction

Porous coordination polymers (PCPs), a class of materials that includes metal-organic frameworks (MOFs),[1–4] are composed of inorganic clusters linked together by organic ligands into 1D, 2D or 3D-networks. These materials have attracted enormous attention in recent years due to their superlative porosity, wide chemical tunability, and their stability. They are being explored for a range of applications including gas storage, gas separation, and catalysis.[5–8] A number of reports on chromatographic separations in PCPs exist,[9–13] but they do not yet perform on par with existing chromatographic materials likely due to fast diffusion through large interparticle voids in packed beds of the solid and similar configurations. Great improvements in separation efficiency could be achieved by modifying the synthesis of these materials to eliminate inter-particle voids and to decrease the average distance between the pores and the external surface of the PCP. These aims could be achieved in a hybrid material based on macroporous polymer monoliths,[14,15] which are presently a leading commercial material for chromatography.[16,17] Previous attempts to unify these material systems have resulted in PCP or MOF crystals embedded in the polymer matrix.[18,19] These approaches still suffer from relatively slow diffusion into the pore structure relative to diffusion through the polymer monolith due to the low external surface area to volume ratio of the PCP or MOF crystals and the great distance between the crystal surface and the majority of the pore volume. Clearly a different synthetic approach is needed that leads to films or similarly dispersed PCPs or MOFs where the majority of the pores are close to the surface.

Here we report a simple procedure for the synthesis of PCP films on the internal surface of a macroporous polymer monolith with excellent potential for chromatographic separations. Using room temperature solution-based[20,21] methods we grow highly porous iron(III) benzenetricarboxylate (FeBTC) coordination polymer films within poly(styrene-divinylbenzene-methacrylic acid) monoliths. The resulting metal-organic polymer hybrid (MOPH) contains highly porous, well dispersed PCP films. These methods are effective for the preparation of bulk powders as well as capillary columns and are likely applicable to a great number of PCP and MOF structures. We demonstrate the utility of MOPHs by using them to enrich phosphopeptides from digested protein mixtures.

Dr. A. Saeed, Dr. F. Maya, Dr. F. Svec, Dr. D. K. Britt
The Molecular Foundry
E. O. Lawrence Berkeley
National Laboratory
Berkeley, CA 94720, USA
E-mail: DavidKBritt@gmail.com
Dr. A. Saeed, Prof. M. Najam-ul-Haq
Division of Analytical Chemistry
Institute of Chemical Sciences
Bahauddin Zakariya University
Multan 60800, Pakistan
D. J. Xiao
Department of Chemistry
University of California
Berkeley, CA 94720, USA

DOI: 10.1002/adfm.201400116

2. Experimental Section

2.1. Materials

Polyimide-coated 100 µm i.d. fused silica capillaries were purchased from Polymicro Technologies (Phoenix, AZ, USA).

3-(trimethoxysilyl)propyl methacrylate (98%, Sigma-Aldrich, St. Louis, MO) was used for capillary pre-treatment. Styrene (99%, Sigma-Aldrich), divinylbenzene (80%, technical grade, Sigma-Aldrich), methacrylic acid (98%, Mallinckrodt Chemicals, St. Louis, MO), toluene (EMD Chemicals, Gibbstown, NJ) and isooctane (Sigma-Aldrich), were used as the monomers and porogens for column preparation. 2,2′-azobisisobutyronitrile (98%, Sigma-Aldrich) was used as the polymerization initiator. All monomers were purified by passage through a bed of basic alumina to remove the polymerization inhibitors. Iron (III) chloride hexahydrate, benzene-1,3,5-tricarboxylic acid (H_3BTC), acetonitrile (ACN), adenosine-5′-triphosphate (ATP), ammonium bicarbonate, trifluoroacetic acid (TFA, analytical reagent grade) ethanol, iodoacetamide (IAA), dithiothreitol (DTT), mono- and dibasic sodium phosphate, phosphoric acid, 2,5-dihydroxybenzoic acid (DHB) were purchased from Sigma-Aldrich and used as received. Trypsin (bovine pancreas), bovine serum albumin (BSA) and casein (bovine milk) were obtained from Sigma-Aldrich. Nonfat milk was purchased at a local grocery store.

2.2. Porous Polymer Monolith Preparation

A 1 mL glass vial was loaded with 50 mg styrene, 100 mg divinylbenzene, 50 mg methacrylic acid, 300 mg toluene and 300 mg isooctane. 4 mg 2,2′-azobisisobutyronitrile (1% with respect to monomers) was added to initiate polymerization. The mixture was homogenized by sonication for 10 min and degassed by purging with nitrogen for 10 min. The vial cap was sealed with plastic paraffin film. The polymerization was carried out in a water bath at 60 °C for 6 h. After cooling at room temperature the glass vial was broken carefully and the polymer monolith was transferred into a cellulose extraction thimble. Porogens and unreacted compounds were removed by Soxhlet extraction in methanol for 16 h. The products were characterized using nitrogen adsorption, thermogravimetry, FT-IR, and Mössbauer spectroscopy.

Preparation of the polymer monolith was adapted to capillary columns using a modified procedure reported by Svobodova et al.[22] Using a syringe pump the capillary was rinsed with acetone followed by water. 0.2 M aqueous sodium hydroxide was then pumped through the capillary at 0.25 µL/min for 30 min followed by rinsing with water until the effluent was at neutral pH. The capillary was then flushed at 0.25 µL/min with a 0.2 M HCl for 30 min, followed by rinsing with water and ethanol. Finally, a 20% (w/w) ethanol solution of 3-(trimethoxysilyl) propyl methacrylate with an apparent pH adjusted to 5 using acetic acid was pumped through the capillary at a flow rate of 0.25 µL/min for 1 h, to vinyl-functionalize the inner surface of the capillary enabling anchoring of the polymer monolith. The capillary was then washed with acetone, dried in a stream of nitrogen, and left at room temperature overnight before use. The vinyl-functionalized silica capillary was filled with the same polymerization mixture used for the bulk monolith. Both ends of the capillary were carefully sealed with a rubber septum and the thermally initiated polymerization was carried out under the same conditions as for the bulk monolith. The unreacted compounds (mostly porogens) were removed by flushing the column with acetonitrile at 6 µL/min for 30 min.

2.3. Growth of the FeBTC MOPH

For the preparation of bulk MOPH powders the monolith was ground lightly with a mortar and pestle. The resulting powder (100 mg) was immersed in 5 mL of 2 mM $FeCl_3.6H_2O$ in ethanol for 15 min, vacuum filtered using a Nylon filter (0.22 µm), and washed with ethanol. The powder is then immersed in 5 mL of 2 mM 1,3,5-benzenetricarboxylic acid (H_3BTC) in ethanol for 15 min and filtered in the same way. This procedure is repeated as desired; samples in this study were generated by using 10, 20, and 30 cycles, respectively.

For preparation of MOPH within a capillary column the monolithic capillary column was flushed with 2 mM $FeCl_3$ in ethanol for 15 min at 2 µL/min using a syringe pump. It was then flushed with 2 mM H_3BTC in ethanol for 15 min at 2 µL/min. The column was rinsed with ethanol between each step 15 min at 2 µL/min. This procedure is repeated as desired; samples in this study were generated by 5, 10, and 30 cycles, respectively.

2.4. Characterization

Nitrogen adsorption/desorption isotherms at 77 K were measured using an ASAP 2020 surface area and porosimetry analyzer (Micromeritics, Norcross, GA). BET surface area values were calculated using established procedures[23] and pore size distribution was calculated using a non-local density functional theory (NLDFT) method provided by Micromeritics assuming cylindrical pore geometry. Scanning electron micrographs and energy dispersive X-ray spectra of monoliths were obtained using a Zeiss Gemini Ultra Field-Emission Scanning Electron Microscope (Peabody, MA, USA) integrated with an energy dispersive X-ray spectrometer (Thermo Electron, USA). FT-IR spectra of the bulk polymer monoliths were acquired using a Spectrum One IR instrument (Perkin Elmer, Waltham, MA, USA). Mass spectra were obtained by using Bruker Autoflex II MALDI-TOF/TOF. Breakthrough curves and column backpressure measurements were performed with a nanoAcquity UPLC system (Waters, Milford, MA, USA) consisting of a binary solvent pump, sample manager, autosampler, and TUV detector equipped with a 10 nL capillary flow cell. Thermogravimetric analysis was carried out in an air atmosphere using a TA Instruments Q5000IR TGA. Iron-57 Mössbauer spectra were obtained at 77 K with a constant acceleration spectrometer and a cobalt-57 rhodium source. Prior to measurements the spectrometer was calibrated at 290 K with an α-iron foil. All spectra were fit with symmetric Lorentzian quadrupole doublets using the WMOSS Mössbauer Spectral Analysis Software.[24]

2.5. Protein Digestion and Phosphopeptide Enrichment

Proteins were digested using a reported tryptic digestion protocol.[25] Protein (2 mg) was dissolved in 1 mL water and then divided into 200 µL fractions. To each fraction were added 160 µL 1 M ammonium bicarbonate and 50 µL dithiothreitol. The fractions were incubated at 50 °C in a thermomixer for 15 min. Aqueous solution of iodoacetamide (100 mM, 50 µL)

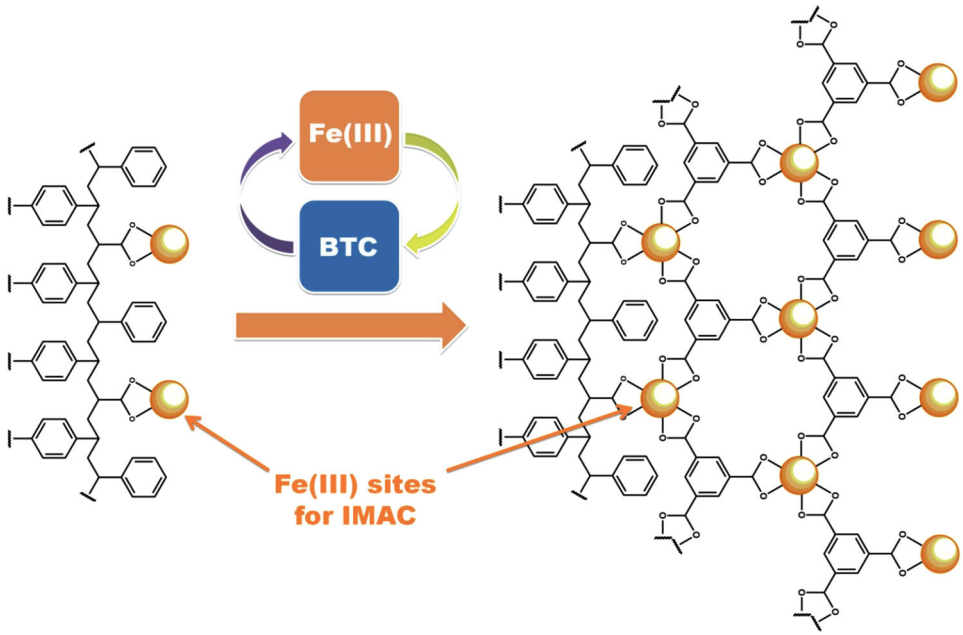

Figure 1. Schematic illustration of incorporation of additional metallic sites for immobilized metal affinity chromatography (IMAC) by step-by-step synthesis of the FeBTC porous coordination polymer into the pore surface of a polymer monolith.

was added gradually while the solution cooled to room temperature. The solution was incubated in the dark for 15 min at room temperature. Deionized water (1 mL) was then added, followed by the addition of 2 µg of trypsin. The protein was then digested in a thermomixer at 37 °C for 14 h. The digestion was terminated by acidifying the solution with 1% TFA (10 µL) and placing it in the thermomixer at room temperature for 5 min. The digested proteins were stored at –20 °C. For the non-fat milk, a sample volume of 0.5 mL was digested using the same procedure as for the other proteins.

Phosphopeptide enrichment experiments were carried out using capillary columns containing native polymer monolith and its MOPH-modified counterpart, respectively. The column was flushed with 100 µL of a 4:1 mixture of acetonitrile and 0.1% TFA for 10 min at a flow rate of 1 µL/min using a syringe pump. Protein digest was then pumped through the column at 2 µL/min for 30 min. To wash out the non-phosphorylated peptides the column was flushed again with a 4:1 mixture of acetonitrile and 0.1% TFA and then with water, both for 10 min at 1 µL/min. Phosphopeptides were eluted using a 250 mM pH 7 phosphate buffer solution pumped at 1 µL/min for 15 min. The eluent was collected in vials and desalted in a commercially available C18 Millipore ZIP-TIP using the standard protocol.[26] A methanolic solution of MALDI matrix (DHB, 2 mg/mL, 2 µL) was then drawn into the tip and the mixture was spotted directly onto the MALDI plate. The spots were analyzed by Bruker Autoflex II MALDI-TOF/TOF. Phosphopeptide peaks were assigned using literature references.[27–31] Column regeneration tests were performed after flushing the column thoroughly with water and then methanol.

Adenosine-5′-triphosphate (ATP) breakthrough experiments were performed by pumping a 1% aqueous acetic acid solution containing 0.25 mg/mL ATP through a 120 mm long MOPH column after 30 cycles of FeBTC growth. ATP concentration in the eluent was determined by UV absorption at 254 nm. Breakthrough capacity is calculated from the elution volume at which concentration C of the eluted ATP represents 50% of the concentration of the original solution C_0 ($C/C_0 = 0.50$).

3. Results and Discussion

3.1. Bulk Monolith Powders

Treatment of a porous poly(styrene-divinylbenzene-methacrylic acid) monolith with successive washes of $Fe(III)Cl_3$ and 1,3,5-benzenetricarboxlyic acid solutions at room temperature results in a metal-organic polymer hybrid wherein a highly porous coordination polymerof iron(III) benzenetricarboxylate is well distributed throughout the pores of the polymer monolith. **Figure 1** provides a schematic illustration of the results of this layer-by-layer growth. After 30 cycles of PCP growth the specific surface area of the FeBTC MOPH is 389 m^2/g, which is nearly four times as large as that of the original polymer monolith, which is 106 m^2/g. N_2 uptake isotherms at 77 K and calculated pore size distribution are presented in **Figure 2**A. The loading of FeBTC and the surface area can be tuned by varying the number of growth cycles (Figure S1 in the Supporting Information). For example, a surface area of 156 m^2/g was obtained after 10 FeBTC MOPH cycles. The pores resulting from growth of the FeBTC coordination polymer are largely below 3 nm in size, as indicated by the pore size distribution calculated from the N_2 isotherm (Figure 2A). This result is consistent with the large increase in N_2 uptake below 0.1 p/p_0.

We examined the distribution of FeBTC within the MOPH using scanning electron microscopy (SEM). As illustrated in Figure 2B the polymer monolith consists of a network of microglobules forming a continuous porous structure. Because

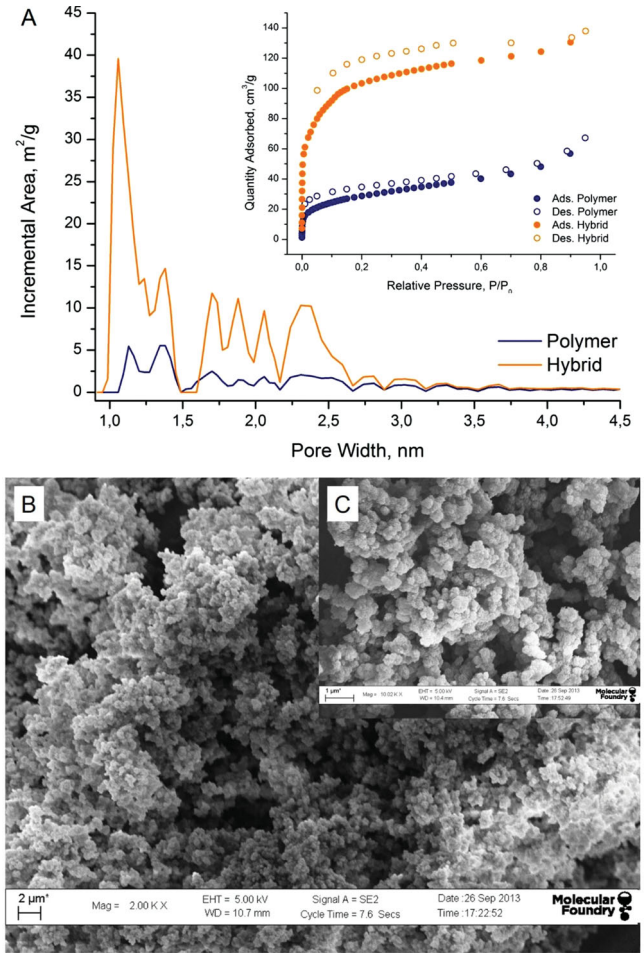

Figure 2. A) Pore size distribution and nitrogen adsorption isotherms of the original polymer monolith and the hybrid polymer monolith after 30 cycles of FeBTC. B) SEM image of the porous structure of the prepared polymer monoliths. C) SEM image of the porous structure of the polymer monolith after 30 cycles of FeBTC.

of its higher reactivity the divinylbenzene polymerizes faster,[32] forming the nuclei of the globules, while the monovinyl monomers, styrene and methacrylic acid, polymerize at a slower rate. The result is a porous structure in which the globules are covered with carboxylic acid groups that can act as nucleation sites for the FeBTC coordination polymer. SEM images of the resulting MOPH (Figure 2C) show that the FeBTC coordination polymer conforms to the surface of the original monolith, leaving the larger meso- and macropores pores intact and available for convective mass transport in flow-through applications.

The FeBTC coordination polymer does not exhibit X-ray diffraction peaks, indicating that it lacks crystalline order. To interrogate its structure we collected FT-IR absorption spectra for the organic polymer monolith and the FeBTC MOPH after 10, 20 and 30 growth cycles (Figure S2 in the Supporting Information). Incorporation of methacrylic acid into the polymer monolith was confirmed by the appearance of an intense band at 1707 cm^{-1} (highlighted in blue), corresponding to the C=O stretch, which is absent in poly(styrene-divinylbenzene) monoliths not containing methacrylic acid (Figure S3 in the Supporting Information). Upon growth of the FeBTC coordination polymer we observe the emergence of absorption bands at 1382, 1449, 1627 and 3400 cm^{-1}. All of these bands increase in intensity with additional cycles of FeBTC growth. These FT-IR bands are consistent with absorption spectra for the metal-organic framework, MIL-100, which is also composed of Fe(III) and trimesate ions.[33]

Given the potential of local structural similarity between the FeBTC material in this report and the MIL-100 framework, we performed Mössbauer spectroscopy on the MOPH prepared with 30 growth cycles to probe the environment of the Fe atoms. As illustrated in the Supporting Information (Figure S4), the Mössbauer spectrum features a set of broad, unresolved quadrupole doublets arising from a mixture of Fe atom environments. While the spectrum is consistent with that of MIL-100,[34] the lack of resolution makes it difficult to eliminate other possible binding geometries.

We also measured the loading of Fe(III) in the polymer monolith using thermogravimetric analysis (TGA) in air on the polymer after one wash with $FeCl_3$ and after 10, 20, and 30 full growth cycles (Figure S5 in Supporting Information). Combustion of the polymer and trimesate ions occurs between 275 and 450 °C, leaving a red inorganic residue. The residue was confirmed to be α-Fe_2O_3 by powder X-ray diffraction. Based on the mass of the Fe_2O_3 residue we calculate the mass percent of Fe in the samples to be 1.1% after one $FeCl_3$ wash, and 1.5, 4.2, and 10.5% after 10, 20, and 30 FeBTC growth cycles, respectively. The small weight loss below 100 °C is attributed to the removal of solvent from the pores of the MOPH; therefore the starting weight in our calculations was taken at 200 °C.

3.2. Capillary Columns

The MOPH synthesis was adapted to capillary columns using standard techniques for preparation of the polymer monolith and alternating pumping of Fe(III)Cl_3 and 1,3,5-benzenetricarboxlyic acid solutions at room temperature with intervening washing steps. We confirmed the immobilization of the FeBTC coordination polymer by energy dispersive X-ray spectroscopy (EDXS) shown in the Supporting Information (Figure S6). The mass percent of Fe in the capillary MOPH after 10 growth cycles is 19%, an order of magnitude higher than the loading observed in the bulk powder after 10 cycles. This difference is due to the forced convection of the precursor solutions through the capillary column, which ensures that the solution fully displaces the existing solvent and completely infiltrates the pore structure. EDXS spectra collected at different points on the capillary column indicate uniform immobilization of FeBTC throughout the column. Spectra collected on different columns prepared with the same number of cycles result in a comparable degree of Fe immobilization.

We determined the total column porosity using high performance liquid chromatography (HPLC) as the ratio of the elution volume of acetone, which is not retained by the column, to the internal volume of the empty cylindrical capillary. The polymer monolith before modification exhibits a total porosity of a 77%, which is consistent with the volume percent of porogens used to prepare the monolith (78.5%). The total porosity decreases

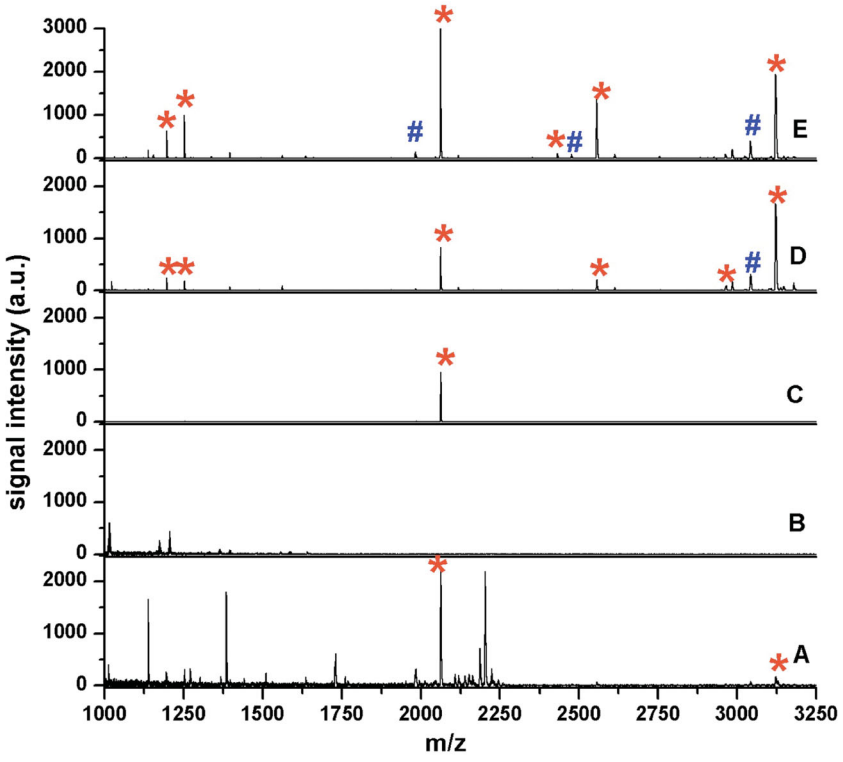

Figure 3. MALDI-TOF-MS spectra of digested β-casein A) before purification and B) after purification using the bare polymer monolith column, C) the polymer monolith after one $FeCl_3$ wash, D) the MOPH after 5 growth cycles of FeBTC, and E) the MOPH after 10 growth cycles of FeBTC. MS peaks resulting from phosphopeptides are indicated with asterisks, while dephosphorylated fragments are indicated with hashes.

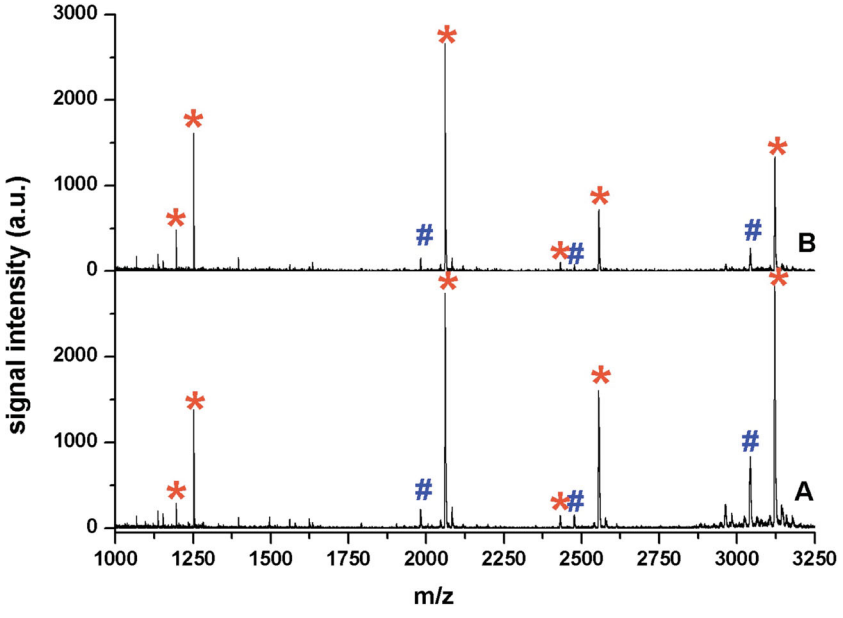

Figure 4. MALDI-TOF-MS spectra of the A) first and B) third digested β-casein samples purified on the same MOPH column prepared with 10 growth cycles of FeBTC, indicating reusability of the MOPH. MS peaks resulting from phosphopeptides are indicated with asterisks, while dephosphorylated fragments are indicated with hashes.

to 72% after 10 growth cycles of FeBTC due to the inclusion of the FeBTC coordination polymer. The reduction in total porosity results in a modest increase in back pressure (Figure S7 in the Supporting Information). Despite this increase, the capillary-based MOPH still enables high flow rates to be used with low-pressure instrumentation, making it an excellent candidate for sample purification.

3.3. Phosphopeptide Enrichment

Solid phase media for immobilized metal-ion affinity chromatography (IMAC) are typically based on silica or polymer beads functionalized with iminodiacetic acid or nitrilotriacetic acid groups, which bind metal ions that confer desired binding selectivity.[35–37] The high abundance of Fe(III) sites in the MOPH materials we report make them excellent candidates for this application. To demonstrate the utility of MOPHs as flow-through media for phosphopeptide enrichment by IMAC we pumped samples of digested proteins through the columns. Phosphopeptides that were retained by the MOPH were eluted using a phosphate buffer and analyzed by MALDI-TOF-MS. **Figure 3**A illustrates the results of enrichment experiments with digested β-casein. The bare polymer (Figure 3B) and the polymer after a single $FeCl_3$ wash (Figure 3C) result in little peptide retention with poor selectivity for phosphopeptides. However, MOPHs with 5 or 10 FeBTC growth cycles (Figure 3D,E, respectively) result in excellent retention and selectivity for phosphopeptides (see Table S1 in the Supporting Information for MALDI peak assignments). We observe the presence of multiple phosphopeptides corresponding to each phosphorylation site in the protein. The recyclability of the MOPH columns was tested by flushing the used column thoroughly with water and then methanol to remove any remaining phosphate buffer. **Figure 4** compares mass spectra of phosphopeptides enriched on the same column in the first and third cycle, indicating no significant change in performance. These results demonstrate the potential of MOPH columns for repeated use.

The potential of the FeBTC MOPH for phosphopeptide IMAC was further tested by increasing the complexity of the sample mixture. **Figure 5** illustrates phosphopeptide enrichment from a digested 1:1:50 mixture of α-casein, β-casein, and bovine serum albumin (BSA) using a MOPH column after 10 FeBTC growth cycles. **Figure 6** shows

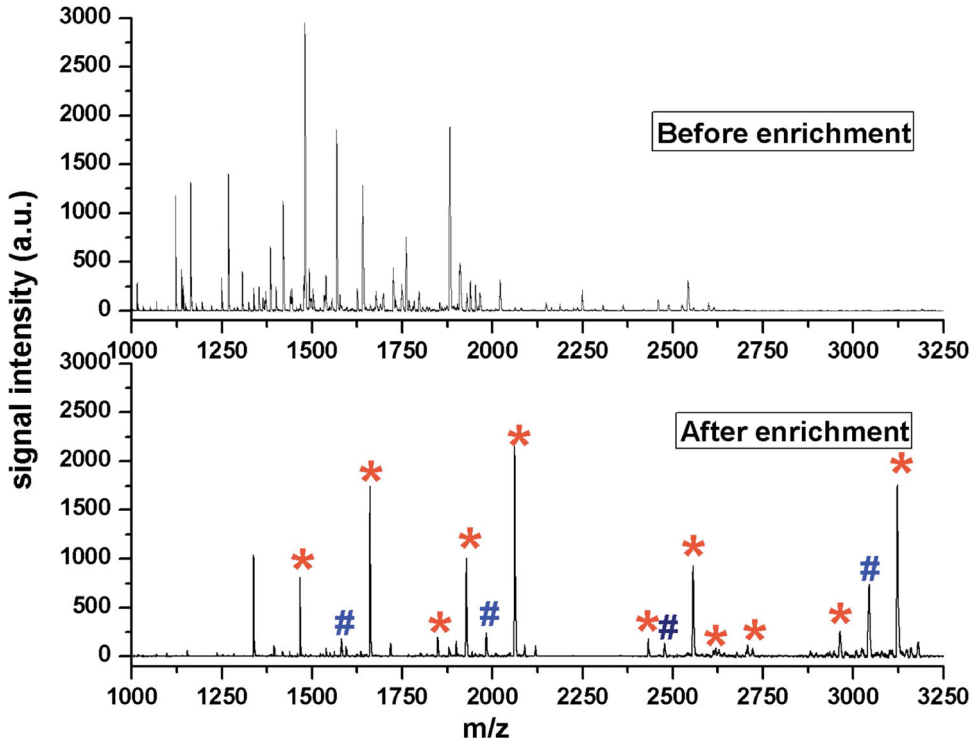

Figure 5. MALDI-TOF-MS spectra of a mixture of digested α-casein, β-casein and BSA (1:1:50) before and after enrichment using a MOPH column prepared with 10 growth cycles of FeBTC. MS peaks resulting from phosphopeptides are indicated with asterisks, while dephosphorylated fragments are indicated with hashes.

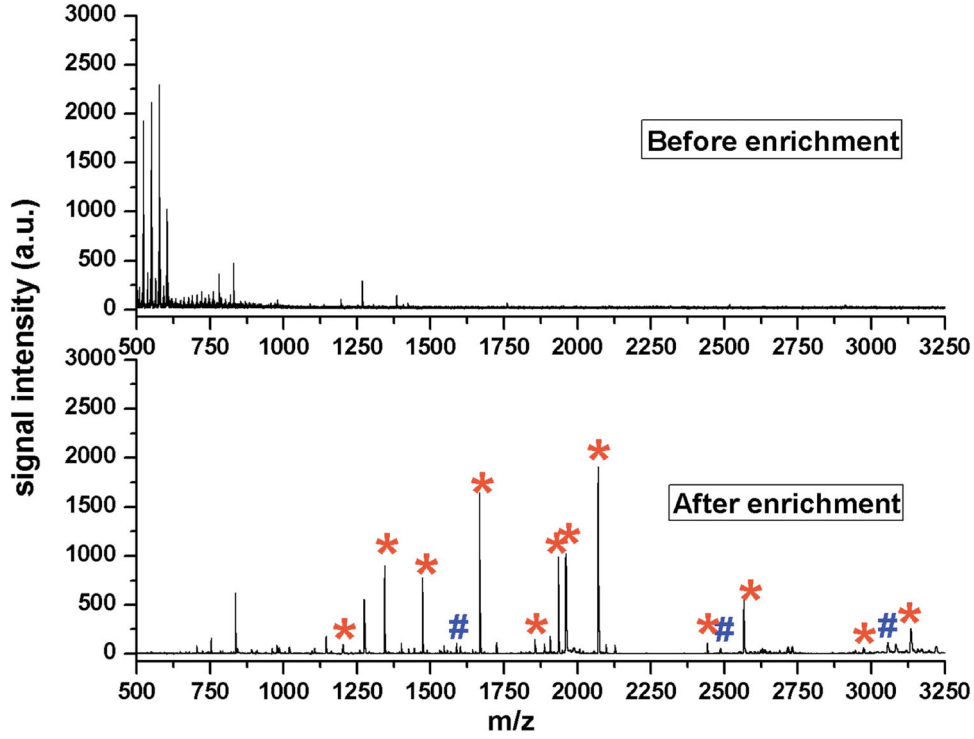

Figure 6. MALDI-TOF-MS spectra of digested nonfat milk before and after enrichment using a MOPH column prepared with 10 growth cycles of FeBTC. MS peaks resulting from phosphopeptides are indicated with asterisks.

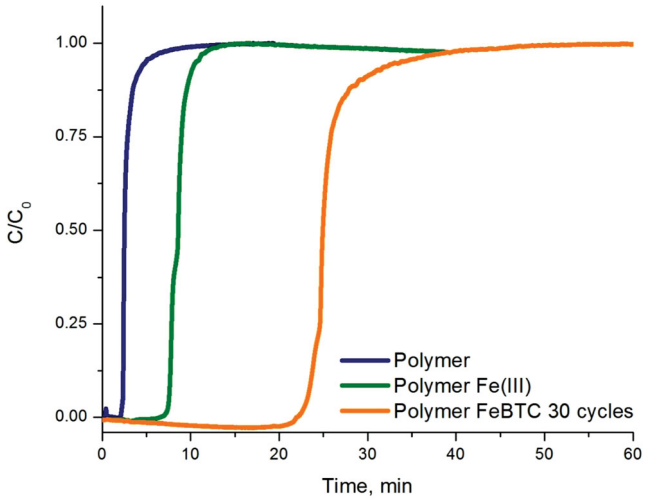

Figure 7. Breakthrough curves of adenosine-5′-triphosphate in the as-synthesized polymer monolith, the polymer monolith after one $FeCl_3$ wash, and the MOPH after 30 growth cycles of FeBTC. The mobile phase is 1% acetic acid in water. Flow rate is 0.5 µL/min. UV detection is at 254 nm. Column length is 120 mm.

phosphopeptide enrichment using a similarly prepared column from digested commercial non-fat milk. In each case the MOPH exhibits remarkable selectivity for phosphopeptides.

We attribute the enhancement in the phosphopeptide enrichment efficiency to the presence of accessible Fe(III) sites on the FeBTC coordination polymer, which are known to bind phosphopeptides selectively. While the local structure around the Fe(III) ions is difficult to determine, a likely structure is the $Fe_3O(CO_2)_6(OH)$ cluster observed in MIL-100 and numerous iron(III) carboxylate coordination polymers.[38,39] The Fe(III) ions in this cluster are coordinated by a labile solvent molecule, constituting a binding site for phosphate.

The high density of Fe(III) sites in the MOPH also suggests that these materials could be employed in preparative scale HPLC purification of phosphopeptides. To achieve a rough estimate of the capacity of the FeBTC MOPH for phosphopeptides we performed breakthrough experiments using adenosine-5'-triphosphate (ATP) as a proxy for phosphopeptides. Breakthrough curves for the bare polymer, the polymer after washing with $FeCl_3$, and the MOPH after 30 growth cycles are shown in **Figure 7**. ATP was not retained in the as-prepared polymer, yielding similar elution time as observed for other non-retained compounds, such as acetone. The observed time at 50% breakthrough in this material is subtracted from the breakthrough time in the iron-containing columns to determine their ATP capacity. The column volume is taken to be the total pore volume in the MOPH. The polymer monolith after one wash of $FeCl_3$ has a capacity of 0.82 µmol ATP/mL. The FeBTC MOPH after 30 growth cycles has a capacity of 3.25 µmol ATP/mL. These results suggest that the MOPH modified monolithic columns are superior to commercial materials used for phosphopeptide enrichment, such as iron affinity gels based on nitriloacetic acid, which typically have a capacity of 2–3 µmol ATP/mL.[40]

4. Conclusions

We present a simple procedure for the growth of well distributed, highly porous coordination polymers (PCPs) in a porous monolithic polymer. The resulting metal-organic polymer hybrids (MOPHs) overcome the problems with diffusional mass transport associated with flow through inter-particle voids and penetration into the small pores present in packed beds of porous solids or pre-grown solids dispersed in porous polymers. We have demonstrated the utility of these materials for enrichment of phosphopeptides by immobilized metal-ion affinity chromatography (IMAC). The synthetic methods we report are readily implemented and likely effective for numerous PCPs and similar materials. The automation of the PCP thin layer growth in capillary-based systems is an exciting possibility that could lead to better control over PCP growth and distribution as well as wide application of these materials for liquid phase separations.

Supporting Information

Supporting Information is available from the Wiley Online Library or from the author.

Acknowledgments

This work was performed at the Molecular Foundry, Lawrence Berkeley National Laboratory and supported by the Office of Science, Office of Basic Energy Sciences, Scientific User Facilities Division of the US Department of Energy, under Contract No. DE-AC02–05CH11231. The financial support of F.M. by a ME-Fulbright fellowship and A.S. by Higher Education Commission of Pakistan is gratefully acknowledged.

Received: January 13, 2014
Revised: May 16, 2014
Published online: July 14, 2014

[1] H. Li, M. Eddaoudi, M. O´Keeffe, O. M. Yaghi, *Nature* **1999**, *402*, 276.
[2] O. M. Yaghi, M. O´Keeffe, N. W. Ockwig, H. K. Chae, M. Eddaoudi, J. Kim, *Nature* **2003**, *423*, 705.
[3] C. Janiak, *Dalton Trans.* **2003**, 2781.
[4] S. Kitagawa, R. Kitaura, S. i. Noro, *Angew. Chem. Int. Ed.* **2004**, *43*, 2334.
[5] Y. Q. Lan, H. L. Jiang, S. L. Li, Q. Xu, *Adv. Mater.* **2011**, *23*, 5015.
[6] M. Maes, M. Trekels, M. Bulhout, S. Schouteden, F. Vermoortele, L. Alaerts, D. Heurtaux, Y. K. Seo, Y. K. Hwang, J. S. Chang, I. Beurroies, R. Denoyel, K. Temst, A. Vantomme, P. Horcajada, C. Serre, D. E. De Vos, *Angew. Chem. Int. Ed.* **2011**, *50*, 4210.
[7] J. R. Li, J. Sculley, H. C. Zhou, *Chem. Rev.* 2012, *112*, 869.
[8] H. Furukawa, K. E. Cordova, M. OΓÇÖKeeffe, O. M. Yaghi, *Science* **2013**, *341*.
[9] R. Ahmad, A. G. Wong-Foy, A. J. Matzger, *Langmuir* **2009**, *25*, 11977.
[10] K. A. Cychosz, R. Ahmad, A. J. Matzger, *Chem. Sci.* **2010**, *1*, 293.
[11] Z. Y. Gu, C. X. Yang, N. Chang, X. P. Yan, *Acc. Chem. Res.* **2012**, *45*, 734.
[12] C. X. Yang, X. P. Yan, *Anal. Chem.* **2011**, *83*, 7144.
[13] Y. Y. Fu, C. X. Yang, X. P. Yan, *Langmuir* **2012**, *28*, 6794.
[14] F. Svec, T. B. Tennikova, Z. Deyl, *Monolithic Materials: Preparation, Properties and Applications*, Elsevier, Amsterdam **2003**.

[15] F. Svec, *J. Chromatogr. A* **2010**, *1217*, 902.
[16] Monolithic HPLC Columns, http://www.phenomenex.com/onyx, (accessed July 2014).
[17] Bia Separations, http://www.biaseparations.com/, (accessed July 2014).
[18] Y. Y. Fu, C. X. Yang, X. P. Yan, *Chem. Commun.* **2013**, *49*, 7162.
[19] H. Y. Huang, C. L. Lin, C. Y. Wu, Y. J. Cheng, C. H. Lin, *Anal. Chim. Acta* **2013**, *779*, 96.
[20] O. Shekhah, H. Wang, K. Kowarik, F. Schreiber, M. Paulus, M. Tolan, C. Sternemann, F. Evers, D. Zacher, R. A. Fischer, C. Woll, *J. Am. Chem. Soc.* **2007**, *129*, 15118.
[21] O. Shekhah, L. Fu, Y. Belmabkhout, A. J. Cairns, E. P. Giannelis, M. Eddaoudi, *Chem. Commun.* **2012**, *48*, 11434.
[22] A. Svobodova, T. Krizek, J. Sirc, P. Salec, E. Tesarova, P. Coufal, K. Stulik, *J. Chromatogr. A* **2011**, *1218*, 1544.
[23] K. S. Walton, R. Q. Snurr, *J. Am. Chem. Soc.* **2007**, *129*, 8552.
[24] WMOSS Mossbauer spectral analysis tools, www.wmoss.org, (accessed July 2014).
[25] M. Rainer, H. Sonderegger, R. Bakry, C. W. Huck, S. Morandell, L. A. Huber, D. T. Gjerde, G. K. Bonn, *Proteomics* **2008**, *8*, 4593.
[26] J. Krenkova, N. A. Lacher, F. Svec, *Anal. Chem.* **2010**, *82*, 8335.
[27] F. Jabeen, D. Hussain, B. Fatima, S. G. Musharraf, C. W. Huck, G. n. K. Bonn, M. Najam-ul-Haq, *Anal. Chem.* **2012**, *84*, 10180.
[28] D. Hussain, M. Najam-ul-Haq, F. Jabeen, M. N. Ashiq, M. Athar, M. Rainer, C. W. Huck, G. K. Bonn, *Anal. Chim. Acta* **2013**, *775*, 84.
[29] N. H. Aprilita, C. W. Huck, R. Bakry, I. Feuerstein, G. Stecher, S. Morandell, H. L. Huang, T. Stasyk, L. A. Huber, G. K. Bonn, *J. Proteome Res.* **2005**, *4*, 2312.
[30] C. Y. Lo, W. Y. Chen, C. T. Chen, Y. C. Chen, *J. Proteome Res.* **2006**, *6*, 887.
[31] U. K. Aryal, A. R. S. Ross, *Rapid Commun. Mass Spectrom.* **2010**, *24*, 219.
[32] J. Urban, F. Svec, J. M. J. Frechet, *J. Chromatogr. A* **2010**, *1217*, 8212.
[33] Y. K. Seo, J. W. Yoon, J. S. Lee, U. H. Lee, Y. K. Hwang, C. H. Jun, P. Horcajada, C. Serre, J. S. Chang, *Microporous Mesoporous Mater.* **2012**, *157*, 137.
[34] A. Dhakshinamoorthy, M. Alvaro, P. Horcajada, E. Gibson, M. Vishnuvarthan, A. Vimont, J. M. Gren+¿che, C. Serre, M. Daturi, H. Garcia, *ACS Catal.* **2012**, *2*, 2060.
[35] X. Xu, C. Deng, M. Gao, W. Yu, P. Yang, X. Zhang, *Adv. Mater.* **2006**, *18*, 3289.
[36] C. Pan, M. Ye, Y. Liu, S. Feng, X. Jiang, G. Han, J. Zhu, H. Zou, *J. Proteome Res.* **2006**, *5*, 3114.
[37] Y. C. Li, Y. S. Lin, P. J. Tsai, C. T. Chen, W. Y. Chen, Y. C. Chen, *Anal. Chem.* **2007**, *79*, 7519.
[38] G. Ferey, C. Serre, C. Mellot-Draznieks, F. Millange, S. Surble, J. Dutour, I. n. Margiolaki, *Angew. Chem. Int. Ed.* **2004**, *43*, 6296.
[39] P. Horcajada, S. Surble, C. Serre, D. Y. Hong, Y. K. Seo, J. S. Chang, J. M. Greneche, I. Margiolaki, G. Ferey, *Chem. Commun.* **2007**, 2820.
[40] PHOS-Select Iron Affinity Gel Technical Bulletin https://www.sigmaaldrich.com/content/dam/sigma-aldrich/docs/Sigma/Bulletin/p9740bul.pdf, (accessed July 2014).